

Course 12.812, General Circulation of the Earth's Atmosphere
 Prof. Peter Stone
Section 9: Numerical Models

Phillips Numerical Experiment: We are going to discuss Phillips' (1956) original numerical experiment in some detail. This initial experiment did not use the primitive equations, but made a number of analytical approximations so as to make the problem tractable for mid 1950's computers. He used the Boussinesq approximation, in which thermodynamical inhomogeneities are neglected except in the buoyancy term, and he used the β -plane approximation, in which all curvature effects are neglected except for a linearization of the variations in the coriolis term,

$$f = 2\Omega \sin \theta \cong f_o + \beta y$$

where y is the meridional coordinate, $f_o = 2\Omega \sin \theta_o$, $\beta = \frac{2\Omega \cos \theta_o}{R}$, $\theta_o =$ some typical mid-latitude, $\Omega =$ rate of rotation, $R =$ radius of earth. (This also neglects the vertical component of the rotation vector.) In addition, he assumed hydrostatic equilibrium, an approximation which is still used in General Circulation Models (GCMs) (although the first two approximations are not). We will take these approximations as granted.

Also he assumed quasi-geostrophic motion, i.e.,

$$0 < Ro \ll 1, \quad Ro = \frac{c}{f_o L}, \text{ with a Burger Number, } \mu = O(1), \text{ where}$$

$$\mu = \frac{N^2 H^2}{f_o^2 L^2} = \frac{\alpha g H^2 \left| \frac{\partial \bar{\Theta}}{\partial z} \right|}{f_o^2 L^2}, \quad \Delta T = \text{typical vertical } \theta \text{ variation} \sim H \left| \frac{\partial \bar{\Theta}}{\partial z} \right|, \quad \frac{\partial \bar{\Theta}}{\partial z} = \text{the basic state stratification.}$$

In non-dimensional form the equations are (scale u, v by c ; w by $Ro \frac{H}{L} c$; t by $\frac{L}{c}$; x, y by L ; z by H ; θ by $Ro \Delta T$; p by $\alpha \rho_o g H \Delta T Ro$, where p is the deviation from the static pressure)

$$u = -\mu \frac{\partial \pi}{\partial y}, \quad v = \mu \frac{\partial \pi}{\partial x}, \quad \frac{\partial \pi}{\partial z} = \theta,$$

$$\frac{\partial \theta}{\partial t} + u \frac{\partial \theta}{\partial x} + v \frac{\partial \theta}{\partial y} + w \frac{\partial \bar{\Theta}}{\partial z} = Q,$$

where θ is the potential temperature perturbation $= \Theta - \bar{\Theta}$, and π is the hydrodynamic Exner Function; and

$$\frac{\partial w}{\partial z} = bv + \frac{\partial}{\partial x} \left(\frac{\partial v}{\partial t} + u \frac{\partial v}{\partial x} + v \frac{\partial v}{\partial y} \right) - \frac{\partial}{\partial y} \left(\frac{\partial u}{\partial t} + u \frac{\partial u}{\partial x} + v \frac{\partial u}{\partial y} \right) + F$$

where $b = \frac{\beta L}{f_o Ro}$, Q is diabatic heating, and F is a friction term. (N.B. we have assumed

$F, Q = O(Ro)$.) The w equation can be re-written in terms of the vorticity, ζ ,

$$\zeta = \frac{\partial v}{\partial x} - \frac{\partial u}{\partial y}:$$

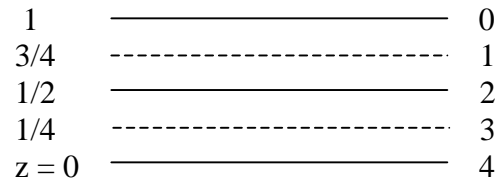
$$\frac{\partial w}{\partial z} = bv + \frac{\partial \zeta}{\partial t} + u \frac{\partial \zeta}{\partial x} + v \frac{\partial \zeta}{\partial y} + \cancel{\frac{\partial u}{\partial x} \frac{\partial v}{\partial x}} + \cancel{\frac{\partial v}{\partial x} \frac{\partial v}{\partial y}} + \cancel{\frac{\partial u}{\partial y} \frac{\partial u}{\partial x}} - \cancel{\frac{\partial v}{\partial y} \frac{\partial u}{\partial y}} + F$$

$$\therefore \frac{\partial w}{\partial z} = bv + \frac{d\zeta}{dt} + F, \text{ where } \frac{d}{dt} = \frac{\partial}{\partial t} + u \frac{\partial}{\partial x} + v \frac{\partial}{\partial y}.$$

The two level approximation is a further approximation to the above equations, which simplifies the vertical variations. For this approximation see Charney and Phillips, (1953).

We divide the atmosphere into layers, as shown in the diagram below, with equal

spacings, $\Delta z = \frac{1}{4}$.



“4” is ground level and “0” the top of the atmosphere. (We are neglecting topography.)

Now we evaluate our u, v and $\frac{\partial w}{\partial z}$ equations at levels “1” and “3”. For all terms not

involving a $\frac{\partial}{\partial z}$, this merely means adding a subscript “1” or “3”. The only $\frac{\partial}{\partial z}$ term is

$$\frac{\partial w}{\partial z}, \text{ and we approximate it by } \left. \frac{\partial w}{\partial z} \right|_1 \cong \frac{w_o - w_2}{z_o - z_2}; \text{ and } \left. \frac{\partial w}{\partial z} \right|_3 \cong \frac{w_2 - w_4}{z_2 - z_4};$$

However, our boundary conditions are $w_o = w_4 = 0$; Also since we have used

dimensionless variables, $z_o = 1, z_2 = \frac{1}{2}, z_4 = 0$.

$$\therefore \left. \frac{\partial w}{\partial z} \right|_1 = -2w_2, \text{ and } \left. \frac{\partial w}{\partial z} \right|_3 = +2w_2.$$

\therefore we obtain the following equations for levels 1 and 3:

(N.B. we are taking $\mu = \text{constant}$, but we could allow it to have different values at different levels.)

$$v_1 = \mu \frac{\partial \pi_1}{\partial x}; \quad v_3 = \mu \frac{\partial \pi_3}{\partial x}; \quad u_1 = -\mu \frac{\partial \pi_1}{\partial y}; \quad u_3 = -\mu \frac{\partial \pi_3}{\partial y};$$

$$-2w_2 = \left(\frac{d\zeta}{dt} \right)_1 + bv_1, \text{ and}$$

$$+2w_2 = \left(\frac{d\zeta}{dt} \right)_3 + bv_3.$$

Finally we evaluate our energy and H.E. equations at level 2:

$$\theta_2 = \left. \frac{\partial \pi}{\partial z} \right|_2 \equiv \frac{\pi_1 - \pi_3}{z_3 - z_1} = 2(\pi_1 - \pi_3); \text{ Also } \left. \frac{\partial \bar{\theta}}{\partial z} \right|_2 = \text{specified constant, and we chose}$$

$$\left. \frac{\partial \bar{\theta}}{\partial z} \right|_2 = 1, \text{ i.e., } \Delta T = H \left| \frac{\partial \Theta}{\partial z} \right| = H \left. \frac{\partial \Theta}{\partial z} \right|_2. \text{ Thus we have}$$

$$2 \left(\frac{\partial}{\partial t} + u_2 \frac{\partial}{\partial x} + v_2 \frac{\partial}{\partial y} \right) (\pi_1 - \pi_3) + w_2 = Q_2.$$

Now we have 7 equations, but 9 unknowns: $u_1, u_2, u_3, v_1, v_2, v_3, \pi_1, \pi_3$, and w_2 . (We can find θ_2 from the H.E. equation, $\theta_2 = 2(\pi_1 - \pi_3)$.) To get around this difficulty we make the simple approximations

$$u_2 = \frac{1}{2}(u_1 + u_3), \quad v_2 = \frac{1}{2}(v_1 + v_3).$$

Thus the two-level model is nothing but a crude two-point numerical integration of the equations with respect to z . Consequently, there would not have been much point to using the more accurate quasi-Boussinesq equations, since they would differ only in the presence of a coefficient depending on z in the $\frac{\partial \pi}{\partial z} = \theta$ equation.

Also, note that we could not have avoided introducing some such approximations as the above ones for u_2 and v_2 by adding the equations evaluated at different levels, because there are always more unknowns than equations, and we can only obtain a determinate

set by introducing some arbitrary relations like those above. Also note that if we had not used the geostrophic approximation, the 7 equations used above would not have been determinate, even with the two assumed relations for u_2 and v_2 . Thus the two-level model is simplest and most useful when we make the quasi-geostrophic approximation.

To analyze his experiment, Phillips looked at the energy cycle. For a quasi-geostrophic two-level model the conversions and energies are:

$$K_M = \frac{1}{2} \int \left([u_1]^2 + [u_3]^2 \right) dy$$

$$K_E = \frac{1}{2} \int [u_1^{*2} + v_1^{*2} + u_3^{*2} + v_3^{*2}] dy$$

$$P_M = 2\mu \int [\pi_1 - \pi_3]^2 dy$$

$$P_E = 2\mu \int [(\pi_1^* - \pi_3^*)^2] dy$$

$$C(P_M, K_M) = 2\mu \int [w_2][\pi_1 - \pi_3] dy$$

$$C(K_E, K_M) = - \int \left([u_1] \frac{\partial}{\partial y} [u_1^* v_1^*] + [u_3] \frac{\partial}{\partial y} [u_3^* v_3^*] \right) dy$$

$$C(P_E, K_E) = 2\mu \int [w_2^* (\pi_1^* - \pi_3^*)] dy$$

$$C(P_M, P_E) = 4\mu \int [\pi_1 - \pi_3] \frac{\partial}{\partial y} [v_2^* (\pi_1^* - \pi_3^*)] dy$$

Note that in this simple model there are very simple relations between the conversions and the total eddy fluxes in the space domain.

Phillips used the above equations as the basis for a numerical integration to see if he could simulate the general circulation of the atmosphere. This calculation is particularly interesting because the manner in which he carried it out, and the analysis of the energetics, give us a possible way of explaining the general circulation in terms of cause and effect.

Since he was going to include finite amplitude effects, he was interested in time scales longer than those appropriate to an adiabatic model, which in general is only valid for $t \sim 3$ days. Thus he had to include dissipative effects, which are not important over periods of a few days, but, being cumulative, are important over periods of a few weeks.

For example, as Jeffries showed, the atmospheric zonal winds, if not maintained by eddies, would be dissipated in $t \sim 12$ days; and changes due to radiative exchange are $\sim 2^\circ/\text{day}$, which, being cumulative, will lead to temperature changes comparable to changes due to advection, which are $\sim 20^\circ/\text{day}$, in $t \sim 10$ days. Consequently in the vorticity equations, Phillips represented the dissipation by

$$F_n = A_v \left(\frac{\partial^2}{\partial x^2} + \frac{\partial^2}{\partial y^2} \right) \zeta_n + v \frac{\partial^2 \zeta}{\partial z^2} \Big|_n$$

For A_v he used the empirical estimate $A_v \sim 10^9 \text{ cm}^2/\text{sec}$. However in a two layer model it is not possible to evaluate a $\frac{\partial}{\partial z^2}$ term, and \therefore he did the following: he assumed that most of the vertical stress occurred near the ground, and could be assumed proportional to the magnitude of the velocity at the ground:

$$\text{Thus } v \frac{\partial^2 \zeta}{\partial z^2} \Big|_1 \cong 0, \text{ and } v \frac{\partial^2 \zeta}{\partial z^2} \Big|_3 = -k \zeta_4.$$

ζ_4 was determined by linear extrapolation from layers 1 and 3, i.e., $\zeta_4 = \frac{3}{2} \zeta_3 - \frac{1}{2} \zeta_1$.

Phillips chose $k = 4 \times 10^{-6} \text{ s}^{-1}$, i.e. a damping time of about 3 days.

In the energy equation, he included a similar diffusion term,

$$Q = A_v \left(\frac{\partial^2}{\partial x^2} + \frac{\partial^2}{\partial y^2} \right) \theta_2 = 2A_v \left(\frac{\partial^2}{\partial x^2} + \frac{\partial^2}{\partial y^2} \right) (\pi_1 - \pi_3)$$

(i.e. he neglected vertical diffusion) with $A_T = A_v$, and a radiation term,

$$Q = -\frac{H}{C_p} \frac{y}{y_0/2}$$

where y is a meridional coordinate with $y = -y_0$ being the equator, $y = +y_0$ being the pole, and H is the mean heating for $-y_0 < y < +y_0$. The value of H and the linear dependence on y are chosen so as to give a crude approximation to the observed radiative heating and cooling rates in the atmosphere. Phillips took $H = 2 \text{ joules}/10^3 \text{ kg}/\text{sec}$. The addition of these terms means that there are now also generation and dissipation terms in the energy equations.

Note that both the radiative heating and the vertical lapse rate of the model are specified a priori. These quantities are actually dependent themselves on the resulting motions, so that by specifying them to have observed values Phillips is really making a consistency calculation to see what circulations arise under these specified conditions. Note that condensation and the hydrological cycle are omitted.

Phillips then integrated these equations in time, numerically, over the rectangular region $0 < x < L$, $-y_0 < y < y_0$. As boundary conditions, he required periodicity in x – i.e.

$f(L) = f(0)$ etc. The equations are 10th order in y , and Phillips broke them up into []

and (*) equations so that they became 20th order. ∴ 5 boundary conditions, applied at $y = \pm y_0$, and at levels 1 and 3, are sufficient. $v = 0 \Rightarrow v^* = 0, [v] = 0$ are two of them.

In addition Phillips specified $[u] = 0$ (which implies $\frac{\partial[\pi]}{\partial y} = 0$) so there is no forcing of

$[u]$ at the boundaries. Finally he specified $\frac{\partial u^*}{\partial y} = \frac{\partial^2 [u]}{\partial y^2} = 0$. These last two are

arbitrary, but we note that that they are fairly weak boundary conditions, not unlike the observed u 's in the atmosphere. A grid of 17(y) x 16(x) points was used. L was taken = 6000km, so eddies larger than this could not develop, and $y_0 = 5000\text{km}$ so

$2y_0 = 10000\text{km} = \text{equator to pole distance}$.

Since the coefficients of the equations are independent of x , if the initial conditions are independent of x , no x dependence will develop – i.e. no eddies. Thus perturbations are necessary to give rise to the eddies (characteristic of instability problems). Therefore Phillips carried out the time integration in two steps. First he started with an isothermal atmosphere at rest and a time step $\Delta t = 1\text{day}$. As a result no eddies formed and a symmetric Hadley cell developed, which reached quasi-equilibrium after 130 days (see figures). This circulation is presumably the circulation that the atmosphere would have on a β -plane if we could “filter” out the eddies. (Realistically the heating function Q would also change if the eddies are removed.) Note however that on a sphere momentum conservation would limit how far the Hadley Cell would penetrate into high latitudes.

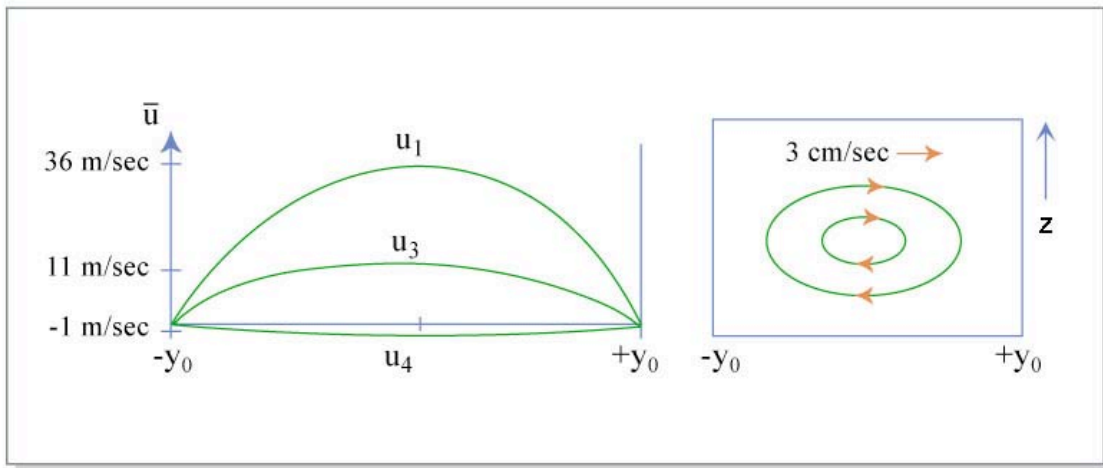


Figure by MIT OCW.

This circulation is qualitatively what one expects for a simple sideways convection problem, with zonal motions created by the coriolis force. In this regime at $t = 130$ days, the energy conversions, in units of $\frac{W}{m^2}$, are $G(P_M) = 5.3, D(P_M) = 0.6,$

$C(P_M, K_M) = 0.05$, $D(K_M) = -0.02$. Thus the system is not in a true equilibrium. The negative dissipation of K_M is because the extrapolated surface wind (u_4) is negative, analogous to the surface easterlies accompanying the Hadley Cell in low latitudes in the real atmosphere. Warm air rising in low latitudes and cool air sinking in high latitudes is creating K_M from P_M , and the motions are predominantly zonal because of the coriolis force.

For the second step, at $t = 130$ days, Phillips introduced a random (non-symmetric) perturbation.

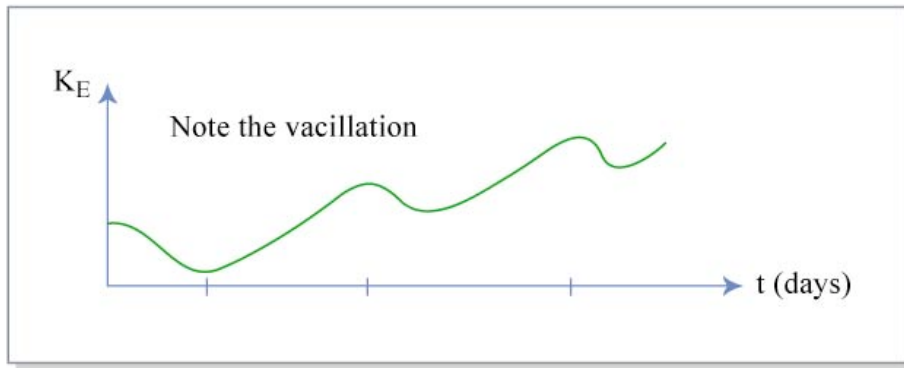
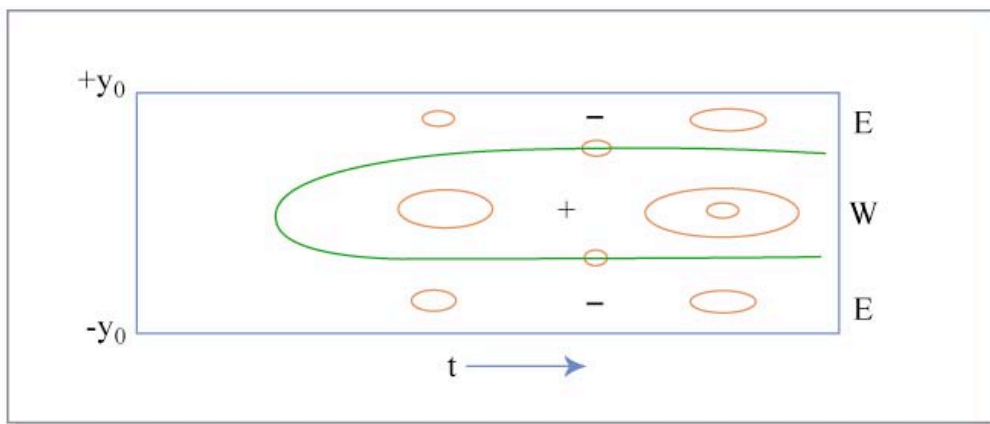


Figure by MIT OCW.

At first K_E decreased, for 5 days, as dissipation smoothed out the initial perturbation. Then a single eddy with wave-length L started to grow, and for the next 20 days the mean flow was irregularly perturbed by this eddy. The resulting flow patterns are remarkably like weather maps. Strong meridional eddy velocities, a 3 celled mean circulation, and surface easterlies and westerlies develop:



Contours of surface zonal velocity, u_0 .

Figure by MIT OCW.

Eventually the integration broke down because of truncation errors, and so the integration was stopped after 31 days and the energetics analyzed for the means over days 5-26, the eddy period. The results are shown in the diagram below. The generation (Q_M) and dissipation (D) terms are included.

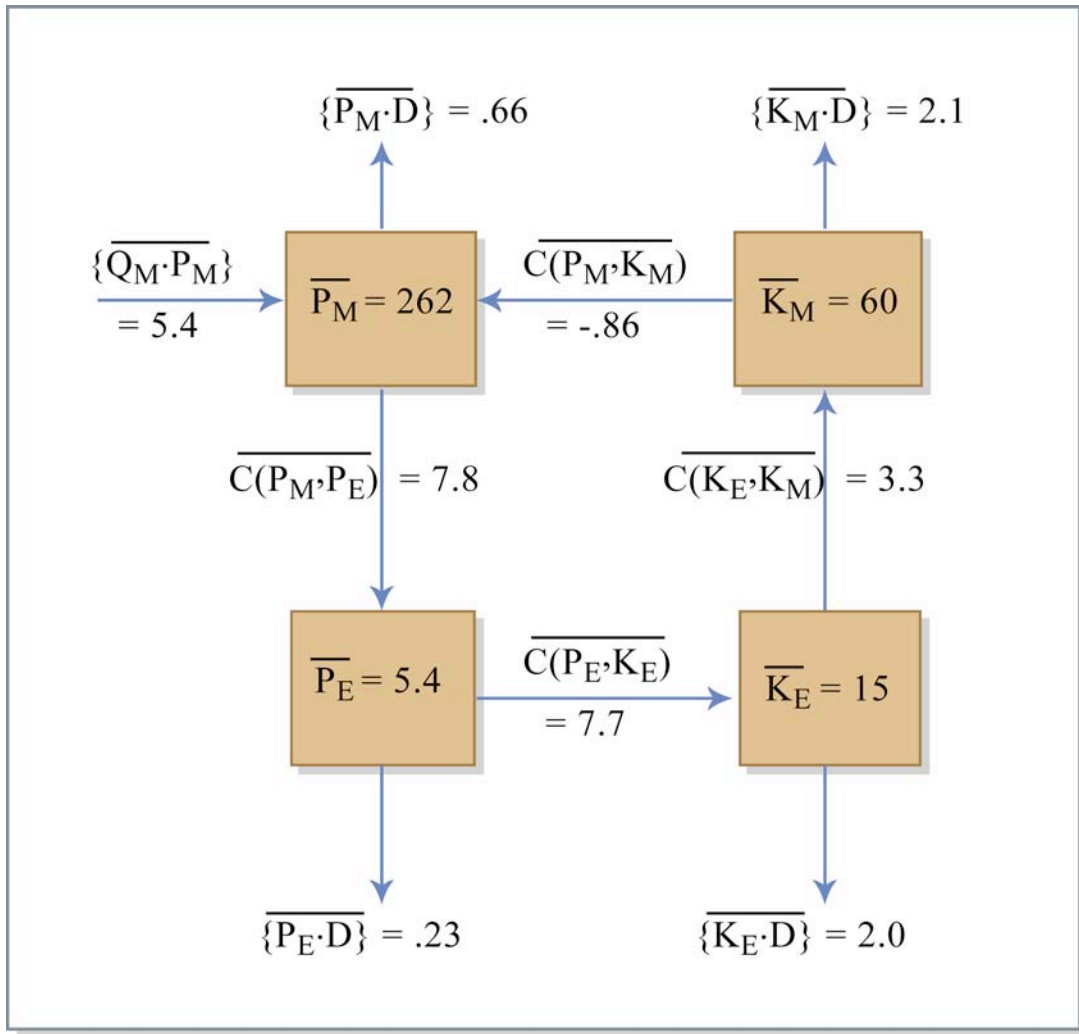


Figure by MIT OCW.

The energy units are 10^5J/m^2 and the conversion units are $\text{W/m}^2 \cong 10^5 \text{J/m}^2/\text{day}$. The bar denotes the time average. Unfortunately, Phillips' definitions of these terms differs from what eventually become standard (he averages zonally first, instead of in time first) and \therefore we cannot compare directly with observations. Nevertheless we can see that the qualitative behavior is similar to the real atmosphere (note that the energy conversions in a 2 level model are less ambiguous than in a P.E. model), i.e.

- 1) Diabatic radiative heating generates P_M ;

- 2) Warm air moving north and cold air south (a net eddy heat transport northward) generates P_E from P_M ;
- 3) Warm air rising and cold air sinking in zonal planes generates K_E from P_E ;
- 4) Eddy transport of momentum into the jet ($u * v *$ correlated with $\frac{\partial \bar{u}}{\partial y}$) generates K_M from K_E ;
- 5) Warm air sinking and cold air rising in meridional planes (the Ferrel cell) generates a small amount of P_M from K_M .

Phillips repeated the experiment with $A_v = 0$. The qualitative behavior was unchanged, although the integration blew up more rapidly.

Thus we get one possible interpretation of the general circulation. The Hadley cell we expect to be driven by differential heating is baroclinically unstable to asymmetric perturbations (which are always present due to topography, etc.) and the asymmetric eddies which arise supply the conversions outlined above. The conversions also show vacillations. Comparing the eddy regime with the Hadley regime, we see that K_M has been increased, and of course the total K , $K_M + K_E$, is increased even more since $K_E = 0$ in the Hadley regime. Since P_M has hardly changed, we see that the “efficiency” of the eddy regime at generating kinetic energy is almost twice as great, which is not surprising since it has more degrees of freedom. Also we see that the direction of the $C(P_M, K_M)$ conversion has been reversed – i.e., the Ferrel cell heat transport downward exceeds the upward transport by the two direct cells in low and high latitudes in the eddy regime. This seems to agree with atmospheric observations (see Oort & Peixoto, 1974), although this conversion is particularly difficult to measure.

Solomon and Stone model (2001): Solomon and Stone used a model more sophisticated than Phillips’, but still quite simplified compared to a GCM, to look at the equilibration problem which Phillips was not able to address. Their model was also a quasi-geostrophic β -plane model, but it has much higher resolution in the vertical – 17 levels, 16 layers with $\Delta p = 62.5\text{mb}$ -- and also it relaxed the quasi-geostrophic assumption of fixed static stability and calculated it interactively. Based on the Stone and Nemet (1996) analysis, these changes are important to resolve the different regimes in the vertical, and to get the baroclinic adjustment due to the vertical eddy heat flux. The equation they solved for the mean static stability, $\theta_s(p)$ in quasi-geostrophic notation, was

$$\frac{\partial}{\partial t} \theta_s = - \frac{\partial}{\partial p} \left(\overline{w^* \theta^*} \right) + \left(\frac{p_o}{p} \right)^k \frac{\tilde{Q}}{c_p} ,$$

where $\overline{(\quad)}$ is a horizontal average over the whole domain as before. Thus $w^*\theta^*$ is no longer neglected. Note that $\theta = \tilde{\theta} + \theta'$, $\tilde{w} = 0$ and $\overline{w'\theta'} = \left[\overline{w^*\theta^*} \right]$. The model is dry.

They also used drag laws for the surface fluxes of SH and momentum, and included the following eddy heat and momentum viscosities in the boundary layer:

$$\nu = \kappa = 5 \left(\frac{p}{p_0} \right)^3 \frac{\text{m}^2}{\text{sec}}, \quad p_0 = \text{surface pressure.}$$

Also a high order friction is included, $F = \nu \nabla^6 \bar{u}$, to remove enstrophy at small scales.

Radiative heating/cooling is simply represented by a Newtonian cooling law,

$$Q = \frac{\theta_e - \theta}{\tau}, \quad \tau = 40 \text{ days,}$$

$$\theta_e = \theta_{ve}(p) + \theta_{he}(y), \quad \text{with } \theta_{ve} \text{ chosen such that}$$

$$\frac{\partial \theta_e}{\partial z} = \begin{cases} -7.0 \frac{\text{K}}{\text{km}}, & \text{in troposphere} \\ 0, & \text{in stratosphere (top 4 layers)} \end{cases},$$

and with $L = \text{channel width} = 10,000 \text{ km}$, and a domain of $0 \leq y \leq L$, in the troposphere they chose

$$\theta_{he} = -21.5\text{K} \sin \pi \frac{y - \frac{L}{2}}{\frac{L}{2}} \quad \text{for } \frac{L}{4} \leq y \leq \frac{3L}{4}, \quad \text{and constant elsewhere. This distribution is}$$

illustrated below.

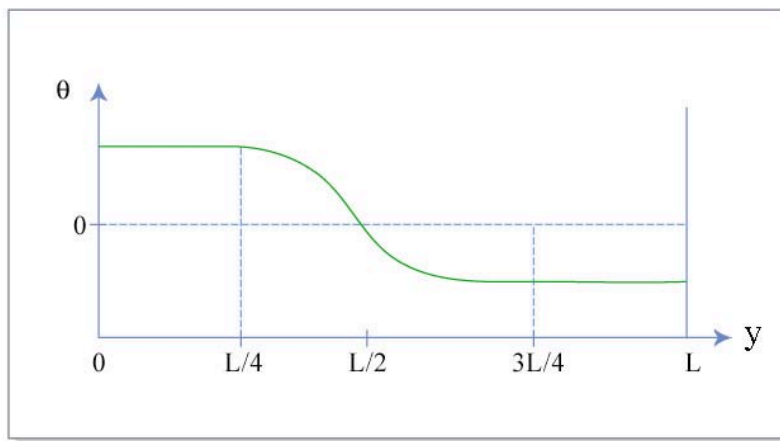


Figure by MIT OCW.

The specified surface temperature is equal to θ_e at $z = 0$. The meridional gradients in the stratosphere are positive and one tenth as strong. The channel is cyclic and 21,040km long. The resolution is ~ 300 km in x, y .

In true R.E. $\frac{\partial T_e}{\partial z}$ would approximately equal -10 K/km in mid-latitudes, and -7 K/km is meant to include the effect of some moist convection.

A standard model run is carried out with parameter choices appropriate to mid-latitude northern winter. It was conducted in a fashion similar to Phillips' experiment. The symmetric state is allowed to develop for 20 days. After 20 days a 3D perturbation with zonal wave numbers 1-9 is introduced. Fig. 8 in Solomon and Stone (2001) shows the evolution of the perturbation potential vorticity in all zonal wave numbers after the perturbation was introduced. We see initial exponential growth in a variety of wave numbers, i.e. instability, with wave number 6 growing most rapidly, followed by wave number 5. Eventually they saturate, and there is a fluctuating equilibrium in which wave numbers 4 and 5 dominate (note the logarithmic scale).

Fig. 5 in Solomon and Stone (2001) shows the evolution of the meridional gradient of the potential vorticity, in units of β . Recall that q is a quasi-conserved quantity, i.e., if $Q = F = 0$, q acts like a tracer, and any mixing would be expected to eliminate gradients in q , i.e., the instabilities will mix q . Also note that in the initial symmetric state in the boundary layer the turbulent mixing implies $\frac{\partial \theta}{\partial z} \sim 0$, while in the troposphere we have a statically stable radiative-convective equilibrium (RCE). With $[u]_{yy}$ neglected, we have:

$$q_y = \beta \left\{ 1 - \frac{1}{\rho_s} \frac{\partial}{\partial z} (h \rho_s) \right\} = \beta \left\{ 1 + \frac{h}{H} - \frac{\partial h}{\partial z} \right\}, \text{ where } h = \frac{f_o^2 \frac{\partial [u]}{\partial z}}{\beta N^2}, \text{ and } h \text{ is proportional to}$$

the slope of isentropes. h decreases with height in the lower troposphere and then levels off. Thus the third term is positive, and $\therefore q_y$ is generally positive in the symmetric state. The symmetric state is still evolving when the eddies are introduced and the effect of the eddies only becomes apparent after about day 12. Since $q_y > 0$, the only source for instability is the temperature gradient at the ground, thus the initial instabilities are classical baroclinic instabilities with $n = 6$ dominating. Furthermore we see that they do mix q , and virtually eliminate q_y in the lower troposphere, i.e., near the steering level, where the amplitude of the eigenmodes is largest. Both the meridional and vertical eddy heat fluxes make important contribution to this homogenization.

But what happens in the equilibrated state? Fig. 3 in Solomon and Stone (2001) shows how the static stability and meridional temperature gradients are changed from the RC equilibrium state by the eddies, along with observations. Qualitatively the changes are realistic. Both the vertical and meridional eddy heat fluxes are dominated by wave 5.

But how is wave 5 maintained? Stability analysis shows that the zonal mean equilibrated state is stable. However stability analysis of the individual waves show that wave 4 when it has large amplitude, is unstable, with the instability being dominated by wave 6. However this wave saturates at low amplitude (see Fig. 12 in Solomon and Stone (2001)) and hands its energy off to larger waves, particularly wave 5. The result is a strong anti-correlation of waves 4 and 5, as shown in the same figure.

Note that this model is still very simple compared to the real world. However, it illustrates that how equilibrium is maintained may not involve classical baroclinic instabilities.

Evaluation of Atmospheric GCMs:

The primary limitation of the models is that there are important small scale processes that cannot be spatially resolved even with the fastest computers available, and thus they must be parameterized. In particular, there is no agreement on what constitutes a proper representation of moist convection and clouds, and virtually every GCM uses different approximations. The result is that the models differ substantially in their simulations of the atmospheric heat balance.

For example, Figure 1 in Gleckler (2005, Geophys. Res. Lett., 32, L15708) shows the wide range of performance of different GCMs that participated in the Atmospheric Model Intercomparison Project (AMIP), both AMIP I and AMIP II. All the models are integrated for 10 years with the lower boundary conditions over the oceans (sea-surface temperatures and sea-ice distributions) specified from observations (1979-1988). The 10 year average surface heat fluxes between atmosphere and oceans were then used to calculate the implied ocean northward heat transport, as in Trenberth and Caron (2001). As shown in Figure 1 of Gleckler (2005), the results are rather poor. For example, the average peak poleward ocean heat transport in the Southern Hemisphere was ~0.2 to 0.3 PW in both AMIP I and AMIP II, whereas observational analyses indicate it should be ~1.5 PW. Note that there was virtually no improvement from AMIP I to AMIP II, in spite of about 10 years of effort to improve the models.

Fig. 3 in Stone and Risbey (1990, GRL, 17, 2173) illustrates the dependence of model vertical heat fluxes on sub-grid scale parameterizations. Changing the moist convection scheme changes the large scale (resolved) vertical heat flux by 50%.

In light of the above, it is not surprising that when many Atmospheric GCMs are coupled to an ocean GCM they cannot simulate the current climate. Typically the ocean circulation collapses, the tropics warm up, high latitudes cool off, the North Atlantic is filled with sea-ice, etc. To get around this many modelers use flux adjustments. First the Atmospheric and Ocean GCMs are run separately with the surface T's specified from observations for the current climate. (In the case of ocean GCMs they are strongly

constrained by using as a surface heat flux boundary condition $H_s = \frac{T_{\text{observed}} - T}{\tau}$ with

τ small. Note that this is an incorrect boundary condition since it implies $H_s = 0$ if the

model reproduces the observed surface T.) The atmosphere and ocean models' "required" fluxes are generally different. For example, if H_A = heat flux into the ocean as simulated by the AGCM, and H_O = heat flux into the ocean as required by the OGCM, then generally $\Delta H = H_O - H_A \neq 0$; in fact often $\Delta H = O(H_A)$. Thus when the models are coupled, frequently ΔH is added to H_A before the heat flux is put into the ocean, i.e., an artificial source (sink) of heat is added at the interface between the atmosphere and ocean, so as to force the coupled model to reproduce the current climate. Similar procedures are followed for the moisture flux and sometimes for the momentum flux. These "adjustments" are then held fixed in climate change experiments.

The main rationale for these adjustments, particularly the adjustments of the heat flux, is that two important feedbacks (the water vapor and ice-albedo-temperature feedbacks) are sensitive to temperature. Thus these feedbacks will not be simulated accurately unless these adjustments are used to force the model to simulate the current climate. However, the adjustments do not in general correct the problem which causes the mismatch in the fluxes in the first place (Marotzke and Stone, 1995, *JPO*, 25, 1350). Mismatches in the surface heat and moisture fluxes are magnified because there are positive feedbacks between the poleward transports in the atmosphere and oceans (Nakamura et al., 1994, *J. Climate*, 7, 1870). Many recent models have simulated surface temperatures that are stable enough that they can be run in climate experiments without flux adjustments, but they still generally have drifts in the ocean, particularly in salinity – e.g., see Figs. 4c, 4d and 5 in Boville and Gent (1998, *J. Climate*, 11, 1115).

Different models also give different results in climate change experiments. The sensitivity of a climate model is generally described by how much its global mean surface temperature increases when the CO₂ concentration in the atmosphere doubles and the system is allowed to reach equilibrium. The IPCC (2001) quoted a range of climate sensitivities of 2 to 5C when atmospheric GCMs are coupled to mixed layer ocean models, with no interactive ocean dynamics. The differences are primarily due to differences in cloud feedback (see below).

Fig. 9.3 in IPCC (2001) summarizes results from coupled Atmospheric/Ocean GCMs for a 1% per year increase in CO₂. Again note the diverse results. The differences are caused not only by different climate sensitivities, but also by different rates of mixing of heat into the deep ocean. Note the natural variability apparent in the figures. Fig. 3 in Forest, et al. (2006, *Geophys. Res. Lett.*, 33, L01705) compares modern coupled GCM performances on these two key factors. The rate of heat uptake in the deep ocean is measured by the global mean of an effective diffusion coefficient which describes how rapidly heat anomalies are mixed below the surface mixed layer by all oceanic processes. The heat uptake differs because of differences in parameterization of sub-grid scale mixing. The rate of heat uptake differs by more than a factor of two between models.

Analyses of differences in atmospheric model feedbacks:

(references: Cess et al., 1989, *Science*, 245, 513-516 and Colman, 2003, *Clim. Dyn.*, 20, 865-873).

Let $G = \text{climate forcing} = -\Delta R = \text{change in TOA net radiative flux out of the climate system} = \Delta I - \Delta Q(1 - \alpha)$ where $\Delta Q(1 - \alpha) = \text{change in absorbed short wave flux}$ and $\Delta I = \text{change in emitted long wave radiation}$.

If G is small enough that the response is linear, then

$$\Delta T_s = \lambda G, \text{ and } \lambda = \frac{1}{\frac{\Delta I}{\Delta T_s} - \frac{\Delta Q(1 - \alpha)}{\Delta T_s}}$$

Where λ is the climate sensitivity parameter. For example, if the emissivity and albedo are constant, then

$$\frac{\Delta Q(1 - \alpha)}{\Delta T_s} = 0, \frac{\Delta I}{\Delta T_s} \equiv \frac{d}{dT}(\epsilon \sigma T^4) = 3.3 \text{ W/m}^2/\text{K} \text{ for the current climate, and}$$

$\lambda \approx 0.3 \text{ K/W/m}^2$. (Note that G is positive, i.e., the flux out of the system is increased when it is warmer.)

Cess et al carried out experiments to compare the climate sensitivity for 14 different GCMs. They were perpetual July experiments with specified SSTs and sea-ice temperatures at the lower boundary (like AMIP). The surface T 's were then changed by $\pm 2\text{C}$, and the differences produced in ΔI and $\Delta Q(1 - \alpha)$ were used to calculate λ . (Note that ice albedo- T feedback has been eliminated.) The data was also used to calculate λ using just F and Q averaged for the clear areas. Call this sensitivity λ_c . The results are shown in Table 2 of Cess et al. (1989).

We see that there is a large range of values for λ , i.e., very different sensitivities, a range of about $2\frac{1}{2}$ times, as in Fig. 3 From Forest, et al. (2006). However, λ_c , which presumably is mainly affected by water vapor feedback, is much more consistent (see the small standard deviation). In fact, the difference between λ and λ_c is directly related to changes in the cloud forcing:

$$\begin{aligned} \text{CF} &= \bar{R} - \bar{R}_{\text{clear}}; \\ \therefore \Delta \text{CF} &= \bar{R} - \bar{R}_c = G_c - G \\ &= \frac{\Delta T_s}{\lambda_c} - \frac{\Delta T_s}{\lambda} = \lambda G \left(\frac{1}{\lambda_c} - \frac{1}{\lambda} \right) = G \left(\frac{\lambda}{\lambda_c} - 1 \right) \end{aligned}$$

$\therefore \frac{\lambda}{\lambda_c} = 1 + \frac{\Delta CF}{G}$; e.g. for a warming, $G > 0$ and $\therefore \Delta CF > 0 \Rightarrow$ an enhanced sensitivity

compared to clear conditions. Recall $CF > 0$ implies clouds warm, so $\Delta CF > 0 \Rightarrow$ enhanced warming, i.e., a positive feedback. Since λ varies considerably between models, whereas λ_c does not, we can conclude that the different model climate sensitivities are primarily due to different cloud feedbacks.

Colman (2003) gives a more up-to-date comparison of model feedbacks, but the conclusion is the same. In his analysis, he distinguishes between feedbacks due to changes in atmospheric water content, in lapse rates, and in ice/snow cover as well as in clouds—see his figure 1. If the changes are small enough, then the feedbacks add linearly. The changes in the first two are strongly anti-correlated, and thus are often added together and referred to as the total water vapor feedback. (Water content and lapse rate are both strongly controlled by the Clausius-Clapeyron equation; thus, when the saturated q increases, q increases and the lapse rate decreases, and this accounts for the anti-correlation between these two quantities.) The anti-correlation causes the sum of the two feedbacks to be robust (see Fig. 1 in Colman, 2003) and thus λ_c is also robust in the models. There is substantial variation in the ice-albedo feedback in the models, but this feedback is relatively small compared to the total water vapor feedback, and to the model-differences in cloud feedback (again see table 1 in Colman, 2003).